Inorganic Chemistry

Article

pubs.acs.org/IC

Dimerization Mechanism of Bis(triphenylphosphine)copper(I) Tetrahydroborate: Proton Transfer via a Dihydrogen Bond

Igor E. Golub,[†] Oleg A. Filippov,[†] Evgenii I. Gutsul,[†] Natalia V. Belkova,[†] Lina M. Epstein,[†] Andrea Rossin,[‡] Maurizio Peruzzini,*[,‡] and Elena S. Shubina*[,†]

[†]A. N. Nesmeyanov Institute of Organoelement Compounds, Russian Academy of Sciences (INEOS RAS), 28 Vavilov Street, 119991 Moscow, Russia

[‡]Istituto di Chimica dei Composti Organometallici Consiglio Nazionale delle Ricerche (ICCOM CNR), via Madonna del Piano 10, 50019 Sesto Fiorentino (Florence), Italy

Supporting Information

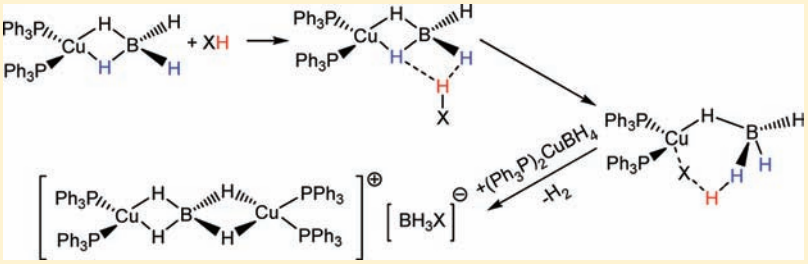

ABSTRACT: The mechanism of transition-metal tetrahydroborate dimerization was established for the first time on the example of $(Ph_3P)_2Cu(\eta^2\text{-}BH_4)$ interaction with different proton donors [MeOH, CH_2FCH_2OH, CF_3CH_2OH, $(CF_3)_2CHOH$, $(CF_3)_3CHOH$, $p\text{-}NO_2C_6H_4OH$, $p\text{-}NO_2C_6H_4N{=}NC_6H_4OH$, $p\text{-}NO_2C_6H_4NH_2$] using the combination of experimental (IR, 190−300 K) and quantum-chemical (DFT/M06) methods. The formation of dihydrogen-bonded complexes as the first reaction step was established experimentally. Their structural, electronic, energetic, and spectroscopic features were thoroughly analyzed by means of quantum-chemical calculations. Bifurcate complexes involving both bridging and terminal hydride hydrogen atoms become thermodynamically preferred for strong proton donors. Their formation was found to be a prerequisite for the subsequent proton transfer and dimerization to occur. Reaction kinetics was studied at variable temperature, showing that proton transfer is the rate-determining step. This result is in agreement with the computed potential energy profile of $(Ph_3P)_2Cu(\eta^2\text{-}BH_4)$ dimerization, yielding $[\{(Ph_3P)_2Cu\}_2(\mu,\eta^4\text{-}BH_4)]^+$.

INTRODUCTION

Metal tetrahydroborates are of great interest because of their potential in hydrogen storage technology,[1−4] as catalysts and selective reducing agents. For example, the title compound, bis(triphenylphosphine)copper(I) tetrahydroborate, is employed as a selective reducing agent for aldehydes,[5] acyl chlorides,[6] and arylsulfonylhydrazones,[7] as a reagent for direct reductive amination[8] in fine organic synthesis, as a photo- and heat-sensitive material,[9] or as a component of solar energy accumulation systems.[10,11]

Despite the existence of a large number of studies dedicated to the structural and dynamic properties[12−15] of transition-metal tetrahydroborates, a thorough investigation of the intermolecular interactions between tetrahydroborates and proton donors has not been carried out yet. In their recent works, Weller et al. have studied the transformations of BH_3NR_3 (R = H and Alk) in a coordination sphere of rhodium and iridium.[16−18] It was shown that NH···HB interactions play a role in lowering the barriers of proton transfer and dihydrogen evolution in these complexes. The first step of the reaction between group 13 hydrides and proton donors was shown as being dihydrogen-bonded (DHB) formation.[19] In this manuscript, we describe the results of a combined computational and spectroscopic study of hydrogen-bonded complexes formed by $(Ph_3P)_2Cu(\eta^2\text{-}BH_4)$ (**1**) with various proton donors and their subsequent transformations. The aim of this work is to reveal the peculiarities in the tetrahydroborate reactivity induced by complexation to a metal.

EXPERIMENTAL SECTION

Dichloromethane (DCM) and tetrahydrofuran (THF) were dehydrated by standard procedures and distilled under argon prior to use. Fluorinated alcohols were provided by P&M (Moscow, Russia). Other reagents were from Sigma Aldrich. The solutions for IR studies were prepared under argon by standard Schlenk technique. IR spectra were measured on a Nicolet 6700 Fourier transform IR spectrometer. Low-temperature IR studies were carried out in the 190−300 K temperature range using a home-modified cryostat (Carl Zeiss Jena). Cryostat modification allows transfer of the reagents (premixed at either low or room temperature) under an inert atmosphere directly

Received: December 2, 2011
Published: June 5, 2012

   dx.doi.org/10.1021/ic202598c | *Inorg. Chem.* 2012, 51, 6486−6497

Scheme 1. Possible Types of Proton-Donor Coordination to Copper Tetrahydroborate

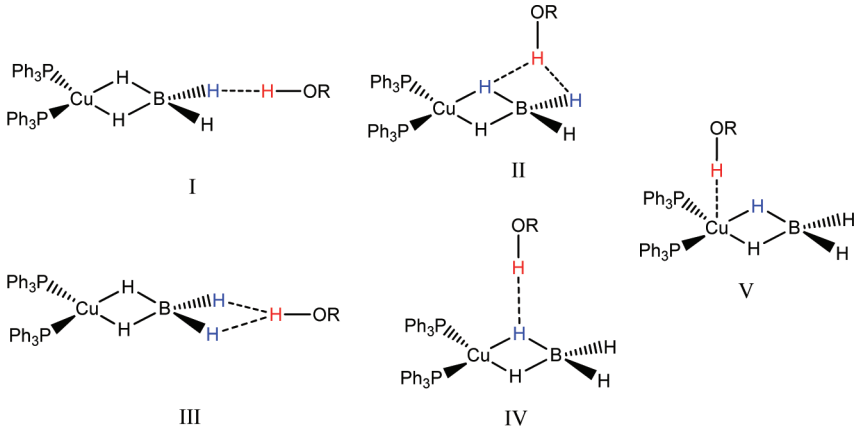

into the cell precooled to the desired temperature. The accuracy of the temperature adjustment was ±0.5 K. For measurements in the ν_{OH} range, the OH acid concentrations were 10^{-2}–10^{-3} M to avoid self-association, whereas $(Ph_3P)_2Cu(\eta^2\text{-}BH_4)$ (**1**) was taken in 10-fold excess. For measurements in the ν_{BH} range, the equimolar ratio or 10-fold excess acids were used. NMR spectra were recorded on a Bruker Avance II 300 MHz spectrometer. ^{1}H chemical shifts are reported in parts per million (ppm) downfield to tetramethylsilane and were calibrated against the residual solvent resonance, while $^{31}P\{^1H\}$ NMR was referenced to 85% H_3PO_4 and ^{11}B NMR to $BF_3{\cdot}Et_2O$.

Variable-Temperature (VT) NMR Experiments on Borohydride Interaction with Trifluoroethanol (TFE). A screw-capped NMR tube was loaded with 20 mg of **1** (0.03 mmol) under an inert atmosphere and then 500 μL (final concentration ca. 0.06 M) of dry and degassed CD_2Cl_2 or THF-d_8 was transferred into the tube via a syringe, under nitrogen. The solutions obtained were first used to record the $^{31}P\{^1H\}$, ^{1}H, ^{11}B, and $^1H\{^{11}B\}$ NMR spectra of the starting material at variable temperatures, by cooling the sample in 20° steps from ambient conditions (300 K) to 190 K. The $^1H\{^{11}B\}$ NMR T_1 values of the BH_4^- ligand in **1** were also measured via the inversion–recovery sequence implemented on the software of the Bruker DRX spectrometer. In a separate experiment, 10 equiv of TFE was syringed into this solution and kept at 190 K in a dry ice–acetone bath. The clear mixtures were then transferred into the NMR spectrometer (already at 190 K) and warmed stepwise to room temperature with the same procedure as that used previously. A new set of multinuclear NMR and $^1H\{^{11}B\}$ NMR T_1 data were recorded during warming and following the reaction course. The H···H distance was estimated by eq 1.[20,21]

$$r_{H\cdots H} = 5.815\left(\frac{1}{T_{1min}^{bonded}} - \frac{1}{T_{1min}^{free}}\right)^{-1/6}\nu^{-1/6} \quad (1)$$

Preparation of Bis(triphenylphosphine)copper(I) Tetrahydroborate (1). The complex was synthesized through modification of the previously described protocol.[22] A total of 10.5 g (0.04 mol) of triphenylphosphine was added to a suspension of 1 g (0.01 mol) of CuCl in 40 mL of CH_2Cl_2, and the resulting mixture was stirred for 3 h at ambient temperature. A solution of 0.8 g (0.02 mol) of $NaBH_4$ in EtOH (7 mL) was then added dropwise, and the mixture was stirred for an additional 1.5 h. The yellow organic layer was washed with H_2O (2 × 50 mL) and dried overnight over $MgSO_4$. After solvent removal, the solid residue was redissolved in a small amount of CH_2Cl_2 and recrystallized from a cold solution (0 °C). The off-white precipitate was washed with 2 × 15 mL of EtOH and 3 × 15 mL of Et_2O to afford 4.6 g of pure bis(triphenylphosphine)copper(I) tetrahydroborate (yield: 76%).

Anal. Calcd for $C_{36}H_{34}BCuP_2$: C, 71.71; H, 5.68; B, 1.79. Found: C, 71.69; H, 5.65; B, 1.85.

IR (cm^{-1}): 2397, 2344, 1987, 1933 (KBr); 2399, 2345, 1989, 1935 (Nujol). ^{31}P NMR (298 K, CD_2Cl_2, δ, ppm): 1.5 (s). ^{1}H NMR (298 K, CD_2Cl_2, δ, ppm): 1.06 (br q, BH_4^-), 7.3–7.4 (multiplet, Ph groups). ^{11}B NMR (298 K, CD_2Cl_2, δ, ppm): −29.7 (quintet, J_{BH} = 79 Hz). The compound is fluxional in the temperature window of solvents used (THF-d_8, CD_2Cl_2); BH scrambling is observed even at 190 K. The BH_4 signal on the ^{1}H NMR spectrum is characterized by one broad quartet that becomes one singlet when decoupled from ^{11}B NMR. This is in line with what was found for other transition-metal borohydride compounds.[23]

Computational Details. Full geometry optimizations were carried out with the *Gaussian09*[24] package at the density functional theory (DFT) level using the M06 functional.[25] The basis sets used were spin-state-corrected s6-31G(d)[26] for the metal center, 6-311G(d)[27] for the phosphorus atoms, and 6-311++G(d,p)[28,29] for the BH_4^- fragment and the alcohol OH group. The 6-31G[28] basis set was used for all other atoms. Frequency calculations were performed for all optimized complexes in the gas phase and reported without the use of scaling factors. The nature of all of the stationary points on the potential energy surfaces was confirmed by vibrational analysis.[30] Transition-state (TS) structures showed only one negative eigenvalue in their diagonalized force constant matrices, and their associated eigenvectors were confirmed to correspond to the motion along the reaction coordinate under consideration using the intrinsic reaction coordinate (IRC) method.[31]

Natural atomic charges and Wiberg bond indices (WBIs)[32] were calculated using the natural bond orbital analysis[33,34] implemented in *Gaussian09*. Topological analysis of the electron-density distribution function $\rho(r)$ was performed using the *AIMALL*[35] program package based on the wave function obtained by the M06 calculations. The energies of H···H interactions were calculated using the correlation between the binding energy ($E_{H\cdots H}$) and the value of the DFT potential energy $V(r)$ in the corresponding critical point (3, −1): $E_{H\cdots H} = 0.5V(r)$.[36,37] Hydrogen-bond ellipticity, ε_{HH}, was defined as $\varepsilon = \lambda_1/\lambda_2 - 1$, where λ_1 and λ_2 are the negative eigenvalues of the Hessian of the electron density at the bond critical point ordered such that $\lambda_1 < \lambda_2 < 0$.[38–40]

The complex formation energy was calculated in the gas phase, taking into account the basis set superposition error (BSSE; by the Bernardi and Boys method);[41] zero-point vibrational energy (ZPVE) correction was determined from the unscaled harmonic frequencies.[42,43]

The inclusion of nonspecific solvent effects in the calculations was performed by using the single-molecule detection method.[44] The interaction energy was calculated in CH_2Cl_2 (ε = 8.93) for the gas-phase-optimized geometries. Changes in Gibbs energies and enthalpies in the solvent were determined using corresponding corrections obtained for the gas phase:[45]

$$\Delta H_{DCM} = \Delta E_{DCM} + \Delta H_{gas}^{corr}$$

$$\Delta G_{DCM} = \Delta E_{DCM} + \Delta G_{gas}^{corr}$$

dx.doi.org/10.1021/ic202598c | Inorg. Chem. 2012, 51, 6486–6497

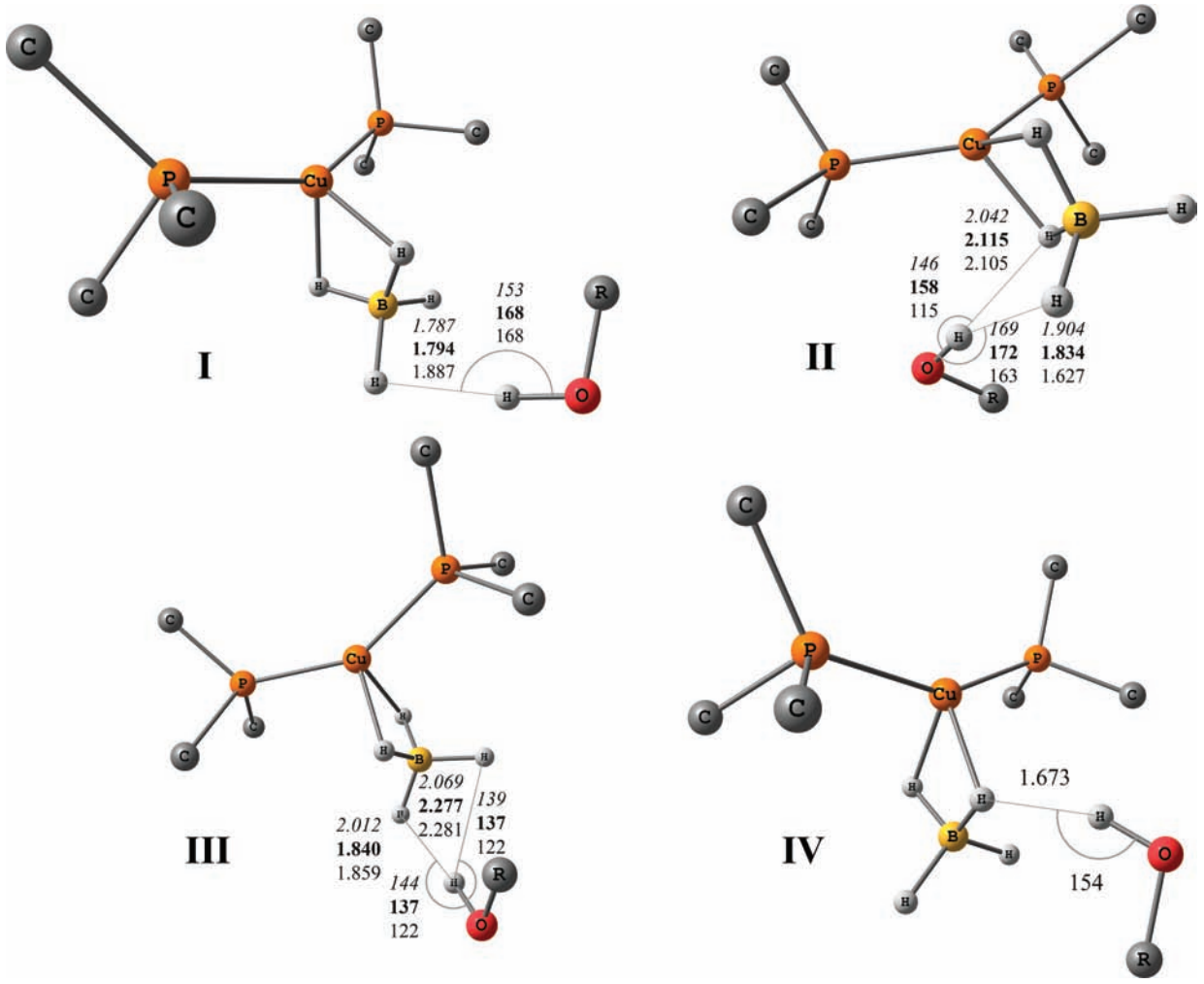

Figure 1. DFT/M06-optimized geometries of DHB complexes between **2** and ROH. The H···H distances (in Å) and OH···H angles (in deg) are for ROH = MeOH (*italic*), TFE (**bold**), and HFIP (regular). Hydrogen atoms of the PMe_3 ligands are omitted for clarity.

RESULTS AND DISCUSSION

Theoretical Investigation of DHB Complexes. *Structural Analysis.* Polyhydrides having hydride ligands of two different types (terminal and bridging) are able to form several hydrogen-bonded complexes. A priori five types of coordination can be envisaged for the hydrogen bonding of alcohols to **1** (Scheme 1). First, we considered the interaction of MeOH with both the "real" complex **1** and its model $(Me_3P)_2Cu(\eta^2\text{-}BH_4)$ (**2**), where phenyl groups were replaced by methyl groups in order to reduce the computational time (Figure S1 in the Supporting Information, SI). No significant change in the geometry and electron-density distribution at the borohydride fragment was found for the model, except for the increase of the P−Cu−P angle by 24°, which makes access to the copper atom less sterically hindered. Consequently, the hydrogen-bonded adduct with MeOH coordination to copper (type **V**, Scheme 1) was found only for **2**. Therefore, further analysis of the interaction with alcohols [MeOH, CF_3CH_2OH (TFE), and $(CF_3)_2CHOH$ (HFIP)] was performed using model borohydride complex **2**; hydrogen-bonded adducts of type **V** were excluded from consideration. Local minima on the potential energy surface corresponding to DHB complexes of types **I**−**III** were found for each alcohol. The type **IV** complex was found for HFIP only.

DHB complexes of types **I**−**III** feature short BH···HO contacts of 1.673−1.859 Å (Figure 1; more detailed structural information is given in the SI). These distances are in the range typical for dihydrogen bonds involving boron hydrides but are somewhat larger than the H···H bond lengths in complexes formed by BH_4^- with the same proton donors (1.553−1.654 Å).[19] Similar to the DHB complexes of the tetrahydroborate anion, the H···H distance shortens with an increase of the proton-donor strength.

In bifurcate complexes of types **II** and **III**, there is an additional longer proton−hydride contact of 2.042−2.115 Å. For the primary contacts in complexes of type **II**, the O−H···H(B) angles vary from 163 to 172°, with the range being typical of hydrogen bonds. At the same time, the secondary O−H···H(B) contacts in type **II** and **III** complexes are rather nonlinear, with angles less than 140°. The overall geometries of primary contacts H···H in these complexes are typical of classical medium-strength hydrogen bonds[46] formed by OH donors and of DHBs formed by transition-metal hydrides or boron hydrides.[47]

Upon DHB formation, the O−H bonds elongate by 0.008−0.020 Å. In complexes **I** and **II** with primary coordination to terminal hydride, the elongation of the corresponding $B-H_{term}$ bonds is 0.003−0.012 Å. Interestingly, DHB formation causes shortening of the bridging $B-H^{br}$ bonds by 0.002−0.019 Å,

dx.doi.org/10.1021/ic202598c | *Inorg. Chem.* 2012, 51, 6486−6497

Table 1. Changes of the NPA Charges Relative to the Isolated Species (Δq), WBI, and Electron Densities at the H···H Bond Critical Point (ρ_c) for DHB Complexes of 2 with Alcohols

complex	Δq[H(O)]^a	Δq[H(B)^{bond}]^b		Δq(BH$_4$)^c	WBI H···H^d	ρ_c au
2·MeOH_I	0.052	−0.008		−0.008	0.009	0.020
2·MeOH_II	0.053	−0.008	−0.013	−0.016	0.007	0.016
2·MeOH_III	0.035	0.003	0.002	−0.031	0.002	0.014
2·TFE_I	0.034	−0.016		−0.050	0.009	0.018
2·TFE_II	0.045	−0.015	−0.031	−0.047	0.010	0.018
2·TFE_III	0.036	−0.017	0.017	−0.045	0.006	0.018
2·HFIP_I	0.037	−0.086		−0.064	0.006	0.017
2·HFIP_II	0.054	−0.017	−0.017	−0.039	0.028	0.028
2·HFIP_III	0.038	0.008	0.001	−0.060	0.007	0.018
2·HFIP_IV	0.033	−0.040		−0.053	0.013	0.023

^{a}Proton of HOR. ^{b}Hydridic hydrogen atom involved in the dihydrogen bond. ^{c}Change of the overall charge on the BH$_4$ fragment. ^{d}For main contact.

independent of their participation in interaction with a proton donor. This is accompanied by the elongation of the Cu−H bonds up to 0.074 Å. Thus, DHB formation induces weakening of the metal−tetrahydroborate interaction and makes the B−H$_{br}$ and B−H$_{term}$ bond lengths more equal.

Electron-Density Analysis. DHB formation entails transfer of the electron density from the proton acceptor to the proton donor and density redistribution within the interacting molecules. These changes can be analyzed using different approaches, namely, natural population analysis (NPA),[33,34] WBIs,[32] and Bader's theory "atoms in molecule" (AIM).[38−40]

Transfer of the electron density, which occurs upon DHB formation, increases the polarization of the interacting BH and OH groups. The charge on the proton of HOR becomes more positive, whereas the charge on the interacting hydridic hydrogen(s) becomes more negative (Table 1). These changes are more pronounced for stronger hydrogen bonds; overall, the negative charge of the BH_4^- fragment increases with an increase of the proton-donor strength.

Within the framework of the AIM theory, a hydrogen bond is characterized by the presence of a (3, −1) critical point that allows one to distinguish it from other types of interaction.[48] Despite the presence of several short intermolecular OH···HB contacts in most of the **2**·HOR adducts, the (3, −1) critical point was found only for the closest contact with the most linear O−H···H(B) arrangement. The presence of secondary interactions causes a deviation of the hydrogen-bond geometry from linearity and is reflected in the values of the H···H bond ellipticity. In the complexes, where a single contact between the proton donor and hydride is suggested by the structural parameters (complexes of types **I** and **IV**), the bond ellipticity varies from 0.101 to 0.274. Such values are typical of hydrogen bonds.[19,49−55] For complexes of types **II** and **III** (which clearly show a bifurcate structure), the bond ellipticity ranges from 0.209 to 0.712. The strength of the primary H···H interaction increases for stronger proton donors, as can be seen from the values of the electron density at the (3, −1) bond critical point of the H···H contact (ρ_c). The ρ_c values range from 0.014 to 0.028 au and are close to those for DHB complexes of the tetrahydroborate anion with MeOH and TFE (0.025−0.032 au),[19] falling in the range typical for hydrogen bonds (0.002−0.034 au).[50,56]

The value of the Laplacian of the electron density at the critical point [$L(r)$; Table S2 in the SI] is negative for all DHB complexes, ranging from −0.010 to −0.017. These values are typical for dihydrogen bonds and indicate both the concentration of the electron density between the two interacting hydrogen atoms and the partial covalent character of dihydrogen bonds as expected.[37,56]

WBI (bond population) is a parameter that characterizes the order of the bond between two atoms.[32] For the DHB adducts **2**·HOR, the values of WBI range from 0.020 to 0.028 for the primary interactions and are negligible (<0.001) for additional contacts. The WBI values for the O−H bond decrease in **2**·HOR, in agreement with the O−H bond elongation; these changes are more pronounced for stronger alcohols (Table S3 in the SI). The change of the WBI values for the B−H$_{term}$ (decrease) and B−H$_{br}$ bonds (increase) correlates well with the changes of the B−H$_{term}$ and B−H$_{br}$ bond lengths (Table S1 in the SI).

Thus, the bond lengths and electron density of the borohydride fragment tend to equalize in DHB complexes **2**·HOR. These changes are more pronounced for more acidic alcohols.

Interaction Energies. The DHB formation energy with correction to ZPVE (ΔE_{ZPVE}) depends on the complex type (**I**−**IV**) and on the proton-donor strength, varying in the gas phase from −5.6 to −17.5 kcal/mol. When BSSE is taken into account, a significant (up to 20%) lowering of the complexation energy was observed, especially for HFIP (Table 2). The solvation effect has a strong influence on the DHB formation energy.[57,58] Taking into account the solvent (CH_2Cl_2) gives lower but more reasonable energies (ΔE_{DCM}; Table 2).

Table 2. Formation Energy for DHB Complexes of 2·HOR (kcal/mol)

complex	ΔE_{ZPVE}	ΔE_{BSSE}	ΔE_{DCM}	$E_{H\cdots H}$, kcal/mol	$\Delta H°(\Delta\nu)^a$
2·MeOH_I	−9.8	−9.6	−2.0	−3.5	−4.0
2·MeOH_II	−7.8	−7.9	−3.2	−2.6	−4.1
2·MeOH_III	−5.6	−5.9	−2.0	−2.3	−2.4
2·TFE_I	−11.1	−8.6	−5.2	−3.0	−3.6
2·TFE_II	−12.3	−9.0	−5.8	−3.0	−4.1
2·TFE_III	−11.0	−9.1	−4.6	−3.2	−2.8
2·HFIP_I	−15.6	−13.1	−4.5	−2.9	−4.0
2·HFIP_II	−17.5	−14.7	−8.3	−5.6	−6.0
2·HFIP_III	−15.7	−13.2	−4.8	−3.2	−4.2
2·HFIP_IV	−15.1	−12.6	−5.4	−4.3	−3.7

^{a}Calculated using computed $\Delta\nu_{XH}$ values according to eq 2[59,60] (vide infra).

dx.doi.org/10.1021/ic202598c | *Inorg. Chem.* 2012, 51, 6486−6497

Interestingly, for type **I** complexes, the $E_{H\cdots H}$, values, delivered from AIM, decrease on going from MeOH to stronger alcohol HFIP. This unusual trend indicates a decrease in the preference for a terminal hydride ligand as the DHB formation site for strong proton donors.

Thus, computations suggest definite dominance of interaction between the proton donor and a terminal hydride ligand. However, a bifurcate complex with two terminal hydrides (type **III**) is the least preferable for all alcohols. An increase of the alcohol strength favors additional interaction with bridging BH (formation of complex **II**) and simultaneous weakening of Cu−H_2BH_2 bonding. These findings are confirmed by the use of stronger proton donors in computations of the reaction mechanism (vide infra).

Frequency Analysis. The most characteristic changes in the IR spectra of hydrogen-bonded complexes of boron hydrides with proton donors are observed in the ν_{OH} and ν_{BH} regions.[19,61] Dihydrogen bonding induces a low-frequency shift of OH stretching vibrations and an increase of their intensity compared with the isolated alcohol. The values of the $\Delta\nu_{OH}$ frequency shifts and OH band intensities computed for DHB adducts **2**·HOR are gathered in Table 3.

Table 3. Computed IR Spectroscopic Characteristics of DHB Complexes 2·HOR

			$\Delta\nu_{BH\ term}$,[a] cm^{-1}		$\Delta\nu_{BH\ br}$,[a] cm^{-1}	
complex	$\Delta\nu_{OH}$, cm^{-1}	$\Delta A_{OH} \times 10^4$, L/(mol cm^2)	$\Delta\nu_{BH1}$	$\Delta\nu_{BH2}$	$\Delta\nu_{BH3}$	$\Delta\nu_{BH4}$
2·MeOH_I	−203	1.2	−4	−4	12	31
2·MeOH_II	−211	2.5	−17	22	−4	56
2·MeOH_III	−109	3.0	−10	−10	41	44
2·TFE_I	−180	3.2	−28	−18	76	99
2·TFE_II	−210	3.7	−39	8	47	123
2·TFE_III	−134	3.4	4	5	53	68
2·HFIP_I	−203	3.5	−31	−12	79	120
2·HFIP_II	−361	4.9	−67	16	89	141
2·HFIP_III	−221	3.8	−68	18	77	112
2·HFIP_IV	−184	5.1	13	14	23	91

[a] $\Delta\nu_{BH1} = \nu_{BH1} - \nu^{s}_{BHterm}$, $\Delta\nu_{BH2} = \nu_{BH2} - \nu^{as}_{BHterm}$, $\Delta\nu_{BH3} = \nu_{BH3} - \nu^{s}_{BHbr}$, and $\Delta\nu_{BH4} = \nu_{BH4} - \nu^{as}_{BHbr}$.

The borohydride fragment in complexes **1** and **2** has a local symmetry of the distorted tetrahedron with the point group C_{2v}. In line with this symmetry, all four BH stretching vibrations are IR-active, two stretching vibrations of the terminal BH bonds (ν^{s}_{BHterm} and ν^{as}_{BHterm}) at 2434 and 2472 cm^{-1} and two stretching vibrations of the bridging BH bonds (ν^{s}_{BHbr} and ν^{as}_{BHbr}) at 2070 and 2052 cm^{-1}, in contrast with the free tetrahydroborate anion (point group T_d), for which only one ν_{BH} is IR-active. Upon DHB formation, a lowering of the BH_4 symmetry occurs, which formally leads to four independent vibrations that keep a "memory" of the original symmetry movements. Herein, we discuss them as independent ν_{BH} modes ($\nu_{BH1} - \nu_{BH4}$).

In **2**·HOR adducts of type **II**, ν_{BHterm} of the terminal hydride involved in DHB undergoes a low frequency shift (from −17 to −67 cm^{-1}; Table 3), whereas ν_{BHterm} of noninteracting terminal hydrides shifts to higher frequencies (from 8 to 22 cm^{-1}). In complex **2**·HFIP_IV, the stretches of both noninteracting BH_{term} undergo a high-frequency shift. It should be noted that in **2**·HOR adducts of type **I** both ν_{BHterm} vibrations shift to lower frequencies, despite the fact that only one hydride is bonded to the proton donor. Both ν_{BHbr} vibrations shift to higher frequencies regardless of the type of coordination, indicating that ν_{BHbr} bands cannot be used to distinguish the DHB complex type in IR spectra.

As stated in the literature,[62,63] the oscillation of the Cu−(μ-H)$_2$−B cycle (Chart 1) ν_{Cu-B} is an intense band appearing at

Chart 1

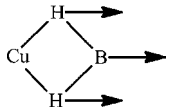

400−300 cm^{-1}. Our calculations give this band at 385 cm^{-1} for **2**. In **2**·HOR complexes, this oscillation appears at 356−391 cm^{-1}, and these values tend to decrease with an increase of the proton donor strength (Table S4 in the SI). The low-frequency shift of ν_{Cu-B} suggests the weakening of the interaction between the copper atom and the BH_4^- fragment as a result of DHB formation, in agreement with the results of the geometry and electron-density analysis.

IR Spectroscopic Study of DHB Formation. Experimentally, DHB formation between **1** and proton donors was studied by VT IR spectroscopy. Monodentate OH acids [MeOH, FCH_2CH_2OH (MFE), TFE, HFIP, $(CF_3)_2COH$ (PFTB), *p*-$NO_2C_6H_4OH$ (PNP), *p*-$NO_2C_6H_4N{=}NC_6H_4OH$ (PNDP)] and bidentate NH acid [*p*-$NO_2C_6H_4NH_2$ (PNA)] were used in solvents of low polarity (DCM and THF) in the temperature range 190−300 K.

In the presence of **1**, the IR spectra of monodentante proton donors in the region of OH stretching vibrations (ν_{OH}) show the appearance of new broad low-frequency bands typical of hydrogen-bond formation (Figure 2). The frequency shift,

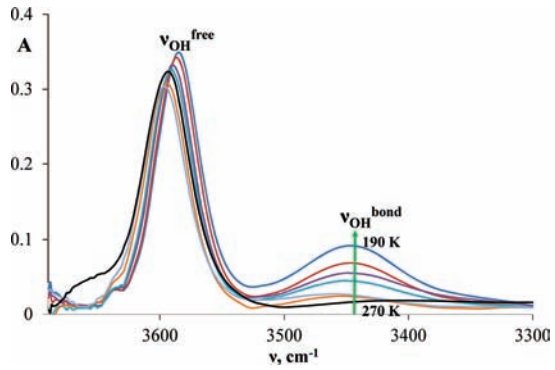

Figure 2. IR spectra in the ν_{OH} region of TFE (0.01 M, black line) in the presence of **1** (0.03 M): CH_2Cl_2, 190−270 K, l = 1.2 mm.

$\Delta\nu_{OH} = \nu_{OH}^{bond} - \nu_{OH}^{free}$, increases with an increase of the proton-donating ability (P_i)[47] of ROH (Table 4). The equilibrium (Scheme 2) shifts toward hydrogen complexes upon cooling, as is evident from the intensity increase of ν_{OH}^{bond} bands. To determine the coordination mode of the bidentante proton donor PNA, analysis of both experimental and computational widths/positions of the two NH bands in the complex was carried out. This approach was successfully applied for complexes of bidentate NH acids with GaH_4^-[63] and AlH_3NMe_3.[64] For the **1**·PNA adduct, the collected evidence suggests a coordination of only *one* NH proton to the hydride (see Figures S3 and S4 and Table S6 in the SI for details).

dx.doi.org/10.1021/ic202598c | *Inorg. Chem.* 2012, 51, 6486−6497

Table 4. Spectroscopic Characteristics of DHB Complexes between 1 and XH Acids

XH	P_i	ν_{XH}^{free}, cm^{-1}	ν_{XH}^{bond}, cm^{-1}	$\Delta\nu_{XH}$, cm^{-1}
PNA	0.41	3501	3480	−87[a]
		3405		
MeOH	0.63	3613	3506	−107
MFE	0.78	3606	3492	−114
TFE	0.89	3590	3448	−142
HFIP	1.05	3568	3351	−217
PNDP	1.23	3546	3240	−306
PFTB	1.33	3520	3206	−314
PNP	1.27	3544	3220	−324

[a]Calculated for a monodentante complex: $\Delta\nu_{NH} = \nu_{NH}^{in\ complex} - [\nu_{NH}^{as} + \nu_{NH}^{s}]/2$.

Scheme 2. DHB Formation Equilibrium

$$(Ph_3P)_2Cu{-}BH_4 + H{-}XR \leftrightarrows (Ph_3P)_2Cu\ {-}BH_4 \cdots H{-}XR$$

The use of Iogansen's empirical correlation (eq 2)[59,60,65,66] allows one to determine the hydrogen-bond formation enthalpy ($-\Delta H_1°$, kcal/mol) from the experimental and theoretical data on ν_{XH} frequency shifts:

$$-\Delta H_1° = \frac{18\Delta\nu_{XH}}{720 + \Delta\nu_{XH}} \quad (2)$$

The enthalpy values obtained from the temperature dependence of the formation constants (eq 3) and from the frequency shift/enthalpy correlation (eq 2) are in perfect agreement. For **1**·HFIP complexes, the thermodynamic parameters determined by these methods are $-\Delta H_1° = 4.2$ kcal/mol, $-\Delta H_2° = 4.2 \pm 0.3$ kcal/mol, and $\Delta S_2° = -16 \pm 2$ cal/(mol K).

$$d\ln K = \frac{1}{R}\left(\frac{-\Delta H_2°}{dT} + \Delta S_2°\right) \quad (3)$$

Analysis of the experimental data in CH_2Cl_2 (Table 5; $-\Delta H°_{exp}$) and of the theoretical data in the gas phase (Table 5; $-\Delta H°_{theor}$) shows that the enthalpies of DHB formation give a linear dependence on the proton-donor strength (determined here as the acidity factor, P_i;[59,60,65−68] Figure 3).

This leads to evaluation of the basicity factor E_j[59,60] (eq 4) as the slope of the $-\Delta H° = f(P_i)$ line. The basicity factor values of the hydride ligands in the gas phase ($E_j = 0.88 \pm 0.04$) and in the solvent ($E_j = 0.91 \pm 0.03$) are the same, in agreement with the independence of E_j from the medium. A comparison of this value with the data for other boron hydrides[59,60,67,69−71] (Figure 4) shows that the basicity of **1** is significantly lower than that of the free tetrahydroborate anion. This can be explained by the decrease of the electron density on the hydride ligands due to coordination of BH_4^- to the copper center. It should be mentioned that the basicity of copper tetrahydroborate **1** is still higher than that of other simple and polyhedral anionic boranes and much higher than that of neutral boron trihydrides.

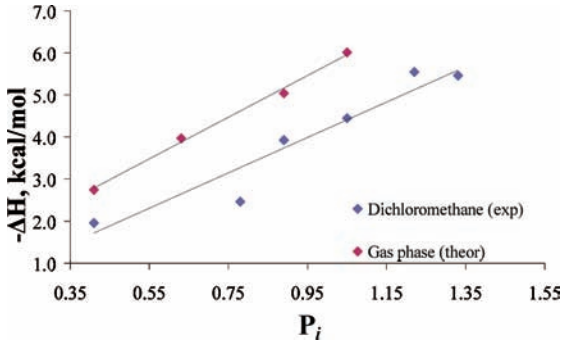

Figure 3. Linear dependence of DHB formation enthalpies ($-\Delta H°$) on the proton-donor strength (P_i) obtained from the experimental data in CH_2Cl_2 (blue points) and the theoretical data in the gas phase (red points).

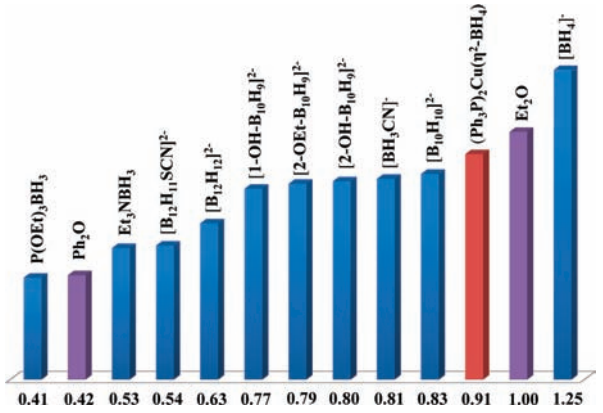

Figure 4. Scale of the basicity factors (E_j) of boron hydrides and some organic bases.

$$E_j = \frac{\Delta H_{exp}}{\Delta H_{11} P_i} \quad (4)$$

DHB and Subsequent Protonation−Dimerization. Investigation of the Mechanism. Formation of a hydrogen bond between **1** and 10 equiv of TFE in both THF and CD_2Cl_2 does not lead to a noticeable shift of the BH_4 signal in low-temperature ^{1}H NMR spectra ($\Delta\delta \leq -0.01$). Under these conditions, a lowering of $T_{1\ min}$ (210 K) from 61 to 28 ms in CD_2Cl_2 and from 65 to 30 ms in THF is observed. This clearly indicates proton hydride interaction. The H···H distance estimated from these data (1.39 for THF and 1.37 for DCM) seems to be overestimated but in the range of dihydrogen bonds.[21]

Formation of a dihydrogen bond between **1** and proton donors (TFE and PNP) in THF leads to the appearance of a new lower frequency ν_{BH}^{bond} band in the region of BH stretching vibrations, whereas the ν_{BHbr} and ν_{BHterm} bands

Table 5. Enthalpies of DHB Formation (in kcal/mol) for 1·HX (Experimental) and 2·HX (Computational, Type II Complexes) Obtained Using $\Delta\nu_{XH}$ Values (Eq 2)

XH	PNA	MeOH	MFE	TFE	HFIP	PNDP	PNP	PFTB
P_i	0.41	0.63	0.78	0.89	1.05	1.23	1.27	1.33
$-\Delta H°_{exp}$	2.0	2.3	2.5	3.9	4.4	5.4	5.6	5.5
$-\Delta H°_{theor}$	2.8	4.1	3.5	4.1	6.0	6.1	6.0	7.1

dx.doi.org/10.1021/ic202598c | Inorg. Chem. 2012, 51, 6486−6497

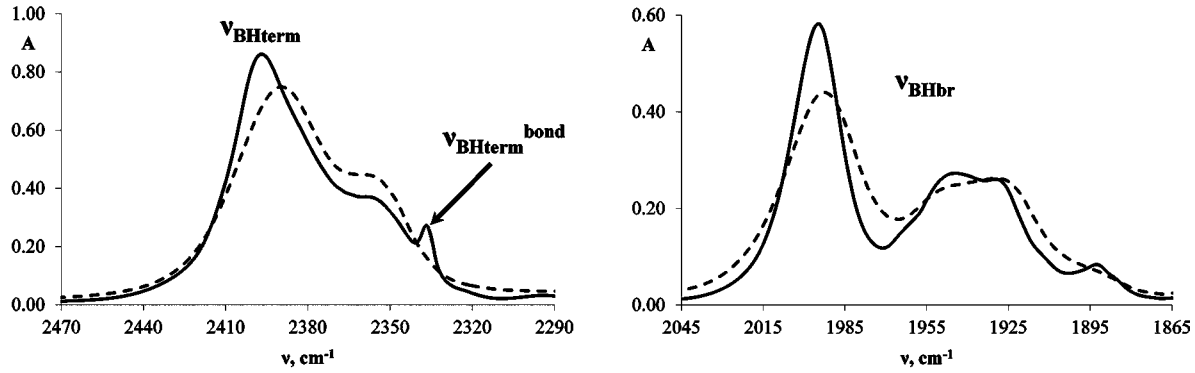

Figure 5. IR spectra in the ν_{BH} region of **1** (0.06 M, dashed line) in the presence of 10-fold excess TFE (0.6 M, solid line): THF, 210 K, l = 0.4 mm.

undergo high-frequency shifts (Figure 5; for spectra at different temperatures, see the SI). Thus, in the presence of 10-fold excess TFE in THF, the initial bands move to ν_{BHterm} = 2386 cm^{-1} ($\Delta\nu$ = 9 cm^{-1}) and ν_{BHbr} = 1990 cm^{-1} ($\Delta\nu$ = 4 cm^{-1}). The new band ν_{BHterm}^{bond} = 2335 cm^{-1} ($\Delta\nu_{BH}$ = −51 cm^{-1}) corresponds to the vibrations of the BH groups involved in DHB. In the presence of 1 equiv of PNP, the new band ν_{BHterm}^{bond} appears at 2339 cm^{-1} ($\Delta\nu_{BH}$ = −47 cm^{-1}). These data definitely indicate the involvement of one of the BH_{term} groups in the interaction with the alcohol. As shown by computations, this DHB could be of type **II**, featuring a hydrogen bond with both terminal and bridging hydrides.

In CH_2Cl_2, the interaction of **1** with an equimolar amount of PNP (or with a 10-fold excess of TFE) at 190−300 K leads to a decrease of the band intensity of terminal and bridging ν_{BH} of both **1** and its DHB adduct; at the same time, a new band at 2124 cm^{-1} appears. The intensity of the new band grows with time irreversibly, and the reaction is accompanied by hydrogen evolution. The new species formed under these conditions could be a dimeric complex of molecular formula $[\{(Ph_3P)_2Cu\}_2(\mu,\eta^4\text{-}BH_4)]^+$ (**3**). This cationic complex with assorted counteranions has already been described in the literature as a product of the reaction between **1** and a strong acid ($HClO_4$ and HBF_4) in alcoholic solvents.[72,73] Herein we obtain it under more mild conditions: in the presence of a rather weak acid, the alcohols or phenols, in a midpolar solvent. According to the literature, the dimer has a single ν_{BHbr} band whose position varies from 2135 to 2150 cm^{-1} depending on the counterion (ClO_4^-, BF_4^-, and PPh_4^-).[72] According to the calculations, the BH_4 fragment in **3** has a local symmetry close to that of the point group T_d and accordingly shows only one intense ν_{BH} band, similar to the free tetrahydroborate anion. Therefore, the band at 2124 cm^{-1} was assigned to the dimeric cationic complex **3**. No NMR data are available from the literature for this dimer. Quantitative conversion of **1** into **3** (at **1**:PNP ratio = 1:1, 5 h at ambient temperature) was confirmed by the complete disappearance of the starting material in IR and NMR spectra. NMR spectra show a new set of signals shifted relative to **1** [$^{31}P\{^1H\}$ NMR at 0.64 ppm ($\Delta\delta$ = −0.61); $^{11}B\{^1H\}$ NMR at −27.82 ppm ($\Delta\delta$ = +2.00)] corresponding to the dimer and a new ^{11}B signal at 2.66 ppm ($\Delta\delta$ = +32.47) assigned to $[BH_2(OC_6H_4NO_2)_2]^-$ species.[74]

In the presence of excess TFE, the reaction is much slower (with 10 equiv of TFE, k_{obs} = (9.0 ± 0.4) × 10^{-7} s^{-1} at 250 K) than in the case of stronger acids (for 1 equiv of PNP, k_{obs} = (6.3 ± 0.1) × 10^{-4} s^{-1} at 250 K), which is in line with the lower formation constant and lower enthalpy of the DHB with TFE. From this evidence, we suggest that the DHB complexes are intermediates of the dimerization reaction. In fact, this reaction was not observed under similar conditions in a THF solution, which could be explained by the lower stabilities and lower formation constants of DHB complexes in this solvent.[19] Another reason may be the interaction of THF with the Lewis center of the copper atom in **1**. Computations support this hypothesis: THF forms a strong complex with **1** having a Cu···O distance of 2.614 Å (ΔE_{ZPVE} = −9.8 kcal/mol; see Figure S9 in the SI).

The kinetics of dimerization was studied by IR spectroscopy at different temperatures on the example of the reaction between PNP and **1**. Representative spectral changes are shown in Figure 6.

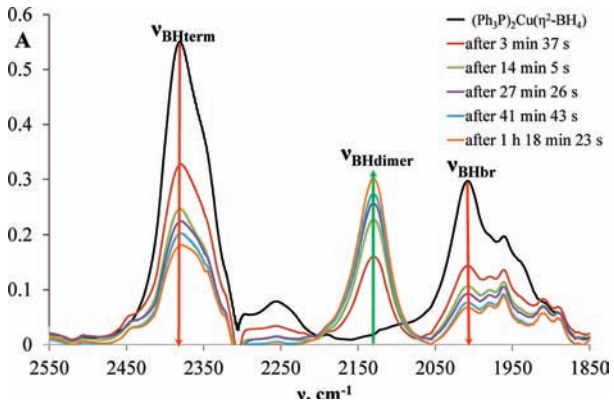

Figure 6. IR monitoring in the ν_{BH} region of the reaction between **1** (0.06 M; black line) and PNP (0.06 M) in CH_2Cl_2 (297 K, l = 0.4 mm) over 78.5 min.

From the kinetic curves (Figure 7), it is obvious that the intensity decrease of ν_{BHterm} and ν_{BHbr} and the increase of the new band $\nu_{BHdimer}$ for **3** occur simultaneously. The changes of the band intensities are caused by the existence of only one rate-limiting step, which is proton transfer. The computational data (vide infra) suggest that the reaction proceeds according to Scheme 3. Because the reaction is accompanied by hydrogen evolution, the last step of the process is irreversible.

$$-\frac{d[a]}{dt} = k_{obs}[a] = \frac{k_2k_3}{k_{-2}+k_3}\frac{K_1[a][b]}{1+K_1[b]} \quad (5)$$

where [a] = [**1**] and [b] = [HX]

$$k_3 \gg k_{-2}; \qquad K_1[b] \ll 1 \Rightarrow k_{obs} \sim K_1k_2[b] \quad (6)$$

dx.doi.org/10.1021/ic202598c | Inorg. Chem. 2012, 51, 6486−6497

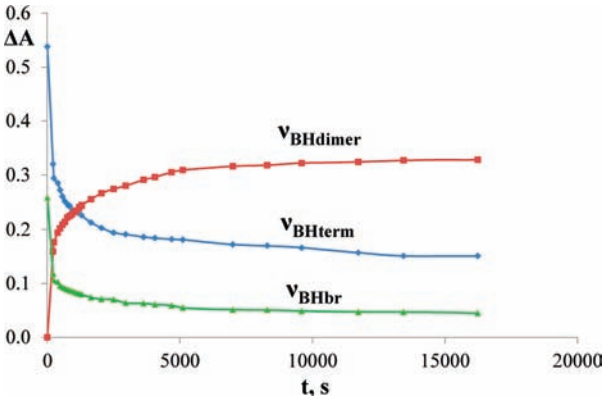

Figure 7. Kinetic curves for the dimerization of **1** in the presence of an equimolar amount of PNP at 297 K: increase of the $\nu_{BHdimer}$ band intensity; decrease of the ν_{BHterm} and ν_{BHbr} band intensities.

Scheme 3. Dimerization Reaction Mechanism

$$(Ph_3P)_2CuBH_4 + H{-}XR \underset{}{\overset{K_1}{\rightleftharpoons}} (Ph_3P)_2CuBH_4 \cdots H{-}XR \underset{k_{-2}}{\overset{k_2}{\rightleftharpoons}} [(Ph_3P)_2Cu]^{\oplus}[BH_3(H_2)XR]^{\ominus}$$

$$[(Ph_3P)_2Cu]^{\oplus}[BH_3(H_2)XR]^{\ominus} \xrightarrow[(Ph_3P)_2CuBH_4]{k_3} [\{(Ph_3P)_2Cu\}_2BH_4]^{\oplus} \| [BH_3XR]^{\ominus} + H_2$$

The kinetic model shown in Scheme 3 is described by eq 5. For small values of the deprotonation constant (k_{-2}) and equilibrium constant (K_1), eq 5 can be simplified to eq 6. The values of the rate constants determined vary from $(8.0 \pm 0.1) \times 10^{-4}$ to $(3.4 \pm 0.1) \cdot 10^{-3}$ s^{-1} in the 195−297 K temperature range (Table S7 in the SI). This gives the reaction activation parameters $\Delta H^{\ddagger} = 3.3 \pm 0.6$ kcal/mol and $\Delta S^{\ddagger} = -59 \pm 2$ cal/(mol K). The significant negative value of the entropy indicates a highly ordered cooperative TS (see Chart 2).[68]

Chart 2

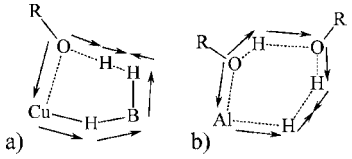

The reaction of proton transfer to the tetrahydroborate anion is well-known.[75,76] The reaction between alcohols and BH_4^- proceeds with DHB complexes as intermediates[19,68,77] with the release of hydrogen. Computational analysis of the reaction energy profile was performed for the model complex **2** interacting with trifluoromethanol (TFM) and with two molecules of *p*-nitrophenol (PNP) as a real proton donor (Figure 8). The acidity and reactivity of the two proton donors are different (gas-phase acidity $\Delta_r H^{\circ}_{acid}$ = 327.9 kcal/mol for PNP[78] and 329.8 kcal/mol for TFM[79]), as is accordingly reflected in the structural and energetic parameters of the reaction intermediates.

The first reaction intermediate was found to be the bifurcate DHB complex of type **II**, with a major interaction with one terminal B−H bond [r(H···H) = 1.672 Å and ∠OH···H = 154° for **DHB_TFM** and r(H···H) = 1.590 Å and ∠OH···H = 172° for **DHB_2PNP**; Figure 9] together with a secondary (weaker) interaction with one bridging B−H bond [r(H···H) = 1.808 Å and ∠OH···H = 135° and r(H···H) = 2.049 Å and ∠OH···H = 120° for TFM and 2PNP, respectively]. Stepwise elongation of the O−H bond led to the TS of protonation (**TS1**). The same structure can be reached by stepwise OH bond elongation in the DHB complex of type **IV**. However, computation of the IRC gave complex **II** as a resting state of proton transfer; thus, only the DHB complex of type **II** should be considered as the intermediate of protonation. DHB complexes of types **I** and **III** did not lead to proton transfer; no local minima of corresponding protonation products were found. Bonding to the bridging hydride ligand seems to help in orienting the alcohol molecule and assists the subsequent formation of the cyclic TS (Cu−O interaction). Therefore, the DHB complexes that do not involve one bridging B−H bond can be regarded as the reaction "dead-ends".

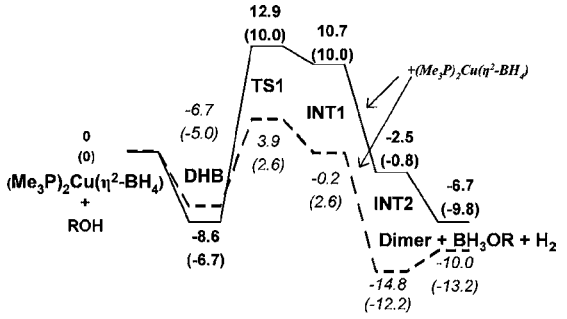

Figure 8. Energy profile for the reaction of **2** with CF_3OH (dashed line, *italic numbers*) and 2 equiv of PNP (solid line, **bold numbers**). The energies [ΔE and ΔH (in parentheses), in kcal/mol] are in CH_2Cl_2 relative to the separated starting molecules. Additional **2** molecules are added at the INT1 and INT2 steps.

The central core of **TS1** can be described as a six-membered ring (Chart 2, a). In other words, it has a cooperative character, where proton transfer from the alcohol to the borohydride is accompanied by coordination of the alcoholate to the copper atom [r(Cu···O) = 2.257 Å for **TS1_TFM** and r(Cu···O) = 2.193 Å for **TS1_2PNP**]. The H_2 ligand formed is relatively strongly bound to both boron and oxygen atoms [r(B−H) = 1.300 Å and r(O···H) = 1.283 Å and r(B−H) = 1.324 Å and r(O···H) = 1.543 Å for TFM and 2PNP, respectively; Figure 9]. The considerable decrease of the proton-transfer barrier on going from PNP to TFM is not surprising because the latter is a stronger acid.

A similar cooperative TS was described recently for the reaction of Me_3NAlH_3 with two MeOH molecules (Chart 2, b),[64] and it was used to explain the extremely easy protonation of aluminum hydride by OH acids. In that structure, the O···H(H) contact was equally short at 1.255 Å. The distance between the oxygen atom of the second MeOH molecule and the metal center [r(Al···O) = 1.889 Å] was shorter than that in the case of **TS1** because of the higher Lewis acidity of aluminum(III) compared with copper(I).

TS1_TFM is found to be 2.6 ($\Delta H^{\ddagger}_{DCM}$) or 3.9 ($\Delta E^{\ddagger}_{DCM}$) kcal/mol above the free reactants in CH_2Cl_2. The enthalpy of **TS1_2PNP** ($\Delta H^{\ddagger}_{DCM}$ = 10.0 kcal/mol) seems to be overestimated relative to the $\Delta H^{\ddagger}$ value obtained experimentally (3.3 kcal/mol). The TS calculations for the real compound (**1**, with Ph groups) give a lower value of 7.8 kcal/mol (Figure S13 in the SI). Quantitative agreement with the experiment is not achieved because calculation of the energy differences in condensed phases, especially when ionic species are involved, is one of the most challenging areas of computational chemistry, but the trend is as expected. Calculated Gibbs free-energy

dx.doi.org/10.1021/ic202598c | *Inorg. Chem.* 2012, 51, 6486−6497

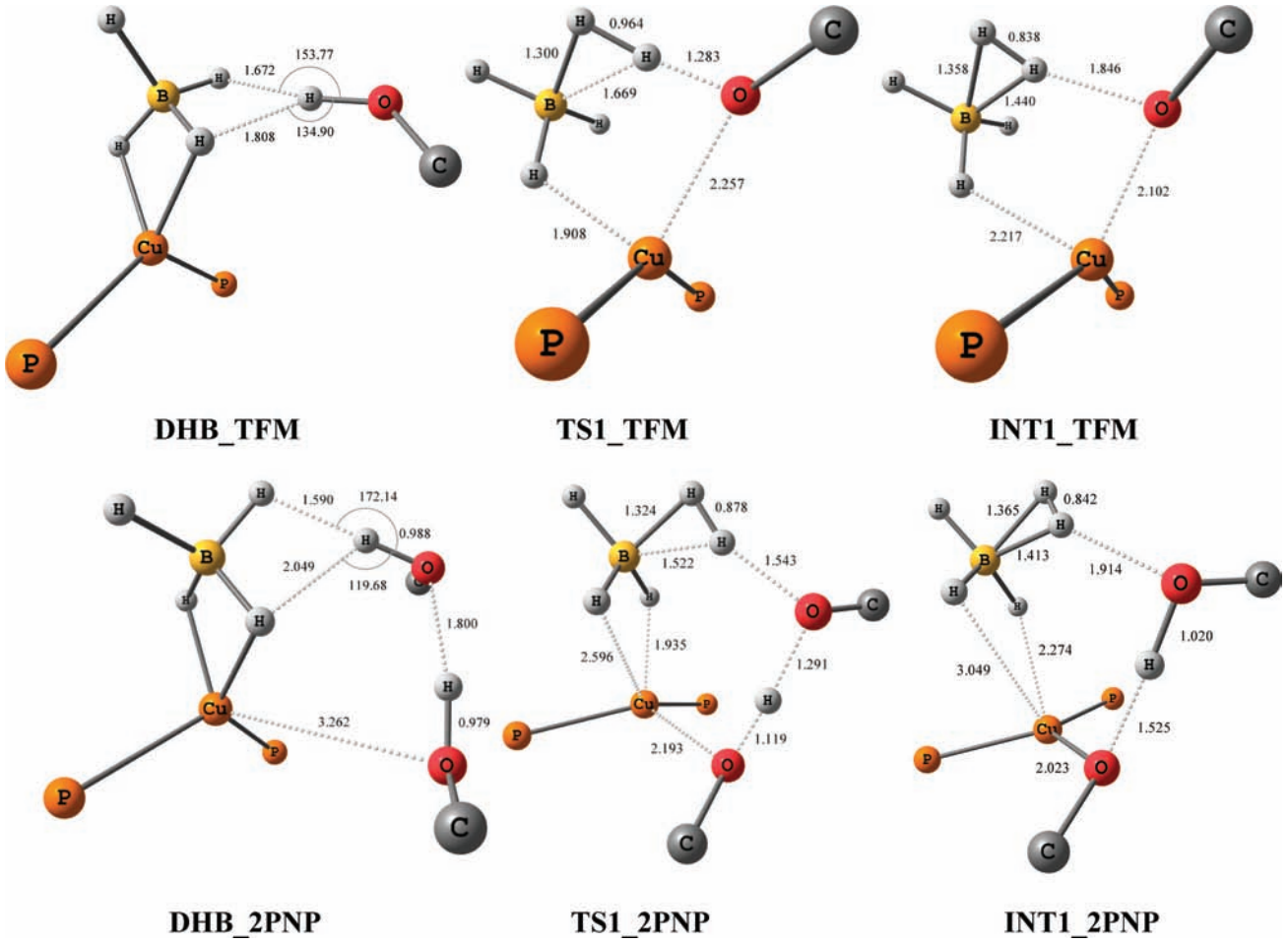

Figure 9. Selected contact lengths and angles for M06-optimized structures of intermediates and TSs of protonation−dimerization. PMe_3 ligands and R of alcohols are omitted for clarity.

values are also in agreement with the experimental data ($\Delta G^{\ddagger}_{DCM,298.15}$ = 17.7 kcal/mol for Me model **2**, $\Delta G^{\ddagger}_{DCM,298.15}$ = 27.5 kcal/mol for Ph compound **1**, and $\Delta G^{\ddagger}_{exp,297}$ = 20.7 ± 2.2 kcal/mol for 4-nitrophenol).

The next local minimum is the protonated intermediate **INT1** composed of the (η^2-H_2)BH_3 unit stabilized by interaction with the [$Cu^+(PR_3)_2(^-OR)$] ion pair (Figure 9). The same (η^2-H_2)BH_3 structures were obtained both experimentally[80,81] and computationally[82] and were proven to be intermediates of the borohydride reaction with strong proton donors.[19] Transition from **TS1** to **INT1** weakens the Cu−HB bond: as the Cu···H(B) distances increase, the Cu···O distance, on the contrary, decreases. So, **INT1** can be described as an alkoxide bis(phosphine)copper complex with a coordinated BH_3(η^2-H_2) moiety. This intermediate is energetically unfavorable; it is located higher relative to initial reagents. Obviously, this unstable complex should undergo further transformations, which might be the elimination of dihydrogen, of the BH_3(η^2-H_2) unit, or of the [BH_3(η^2-H_2)OR]$^-$ fragment, yielding the cationic copper complex (see Figure S11 in the SI). The energies of these reactions for TFM (ΔE_{DCM}) are −12.1, +9.3, and +8.3 kcal/mol, respectively. These data suggest that hydrogen elimination may occur already at this stage. In calculations, we have left the hydrogen molecule coordinated to maintain the integrity of the system under investigation. Nevertheless, the subsequent process should include the simple substitution of a boron-containing fragment in the **INT1** with the second **2** molecule.

To access the dimerization process, we added a second molecule of **2** to **INT1** and obtained another even lower local minimum, **INT2** (the formation energy of **INT2** relative to **INT1** ΔE_{DCM} = −14.6 and −13.2 kcal/mol for **INT2_TFM** and **INT2_2PNP**, respectively; Figure 8). **INT2** features one new Cu−H_{br}(B) bond formation and partial Cu···O bond dissociation. Completion of the Cu···O bond dissociation and formation of a second Cu−H_{br}(B) bond lead to the dimer [{$(Me_3P)_2Cu$}$_2$(μ,η^4-BH_4)]$^+$ (**4**; Figure 10; see also Figure S10 in the SI).

The activation barrier for this process is small and was not found computationally in the gas phase because of accompanying ion-pair dissociation of **4**·[BH_3(η^2-H_2)OR]$^-$. Formation of the dimer **4** is energetically favorable, ΔE_{DCM} = −8.7 kcal/mol relative to the initial reagents for 2PNP, even without taking into account the formation of ion pair **4**·[BH_3(η^2-H_2)OR]$^-$ and elimination of dihydrogen. It is evident that in solution the reaction product **3** should exist as an ion pair, which would provide an additional gain in the reaction energy. In the case of TFM, the dimer **4** has slightly higher energy than **INT2_TFM**, again because of the neglected ion-pair formation. Subsequent elimination of a dihydrogen molecule from the [BH_3(η^2-H_2)OR]$^-$ anion leading to the **4**·[BH_3OR]$^-$ ion pair does not have any effect on the dimerization process mechanism itself. The overall reaction (Scheme 2) is thermodynamically favored

dx.doi.org/10.1021/ic202598c | Inorg. Chem. 2012, 51, 6486−6497

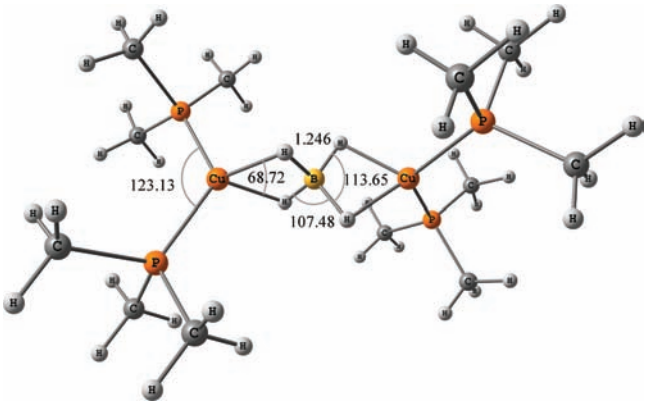

Figure 10. M06-optimized structure of **4**.

(ΔG_{DCM} = −8.9 and −4.8 kcal/mol for reactions with **TFM** and **2PNP**, respectively).

CONCLUSIONS

Dimerization of transition-metal tetrahydroborates, M(η^2-BH_4), in acidic media is known to yield (μ,η^4-BH_4) bridges linking two transition-metal atoms.[72,73,83−86] The combination of experimental (IR, 190−300 K) and quantum-chemical (DFT/M06) methods allowed us to study for the first time the reaction mechanism, taking **1** as the example. The first reaction step is shown to be DHB formation. The subsequent proton transfer yields a [BH_3(η^2-H_2)]-containing copper complex as the next intermediate, which evolves dihydrogen and allows dimer formation.

The structures of different mono- and bifurcate DHB complexes were thoroughly analyzed. As occurred, even in the presence of several short OH···HB contacts, all of the DHB complexes feature only one (3, −1) critical point belonging to the shortest intermolecular contact. Additional interactions lead to an increase of the H···H bond ellipticity. The thermodynamic characteristics of the DHB complexes in CH_2Cl_2 and in the gas phase (from quantum-chemical calculation) and in CH_2Cl_2 and THF (from IR spectra) indicate that the hydride basicity in **1** is substantially reduced as the result of tetrahydroborate coordination to the metal (E_j = 0.91 and 1.25 for **1** and free BH_4^-, respectively). For stronger proton donors, the bifurcate DHB involving both bridging and terminal hydridic hydrogen atoms becomes thermodynamically preferred. Participation of the bridging hydrogen in the interaction with the proton donor turns out to be a prerequisite for the subsequent proton transfer to occur.

Protonation of the tetrahydroborate **1** accompanied by dihydrogen evolution yields the cationic complex **3**. In contrast to the literature data, the reaction occurs in the presence of rather weak acids, such as TFE. According to the calculations, protonation proceeds through a cyclic TS featuring proton coordination to terminal hydride and interaction between the proton donor's oxygen and copper. The simultaneous presence of these interactions has a synergistic effect and accounts for an easier proton transfer to **1** compared with free BH_4^- despite the lower basicity of **1**. In both cases, dihydrogen evolution takes place from the [BH_3(η^2-H_2)OR]$^-$ moiety, whereas the [$(Ph_3P)_2Cu$]$^+$ cation is stabilized by coordination of the second **1** molecule to yield the dimer **3**. The computational results are in good agreement with the experimental kinetic data. They show that the rate-determining step in the process is proton transfer (with a highly ordered TS). This mechanism could be generalized to describe dimerization of other transition-metal tetrahydroborates as well.[72,73,83,85,86]

ASSOCIATED CONTENT

Supporting Information

Optimized geometries (Cartesian coordinates) for the calculated species, detailed computational results, AIM analysis, in-depth analysis of PNA complexes, and kinetic data. This material is available free of charge via the Internet at http://pubs.acs.org.

AUTHOR INFORMATION

Corresponding Author

*E-mail: shu@ineos.ac.ru (E.S.S.), maurizio.peruzzini@iccom.cnr.it (M.P.). Fax: +7 495 1355085 (E.S.S.), +39 055 5225 203 (M.P.).

Notes

The authors declare no competing financial interest.

ACKNOWLEDGMENTS

The authors thank the Russian Foundation for Basic Research (Project 10-03-00960) and the CNR−RAS bilateral agreement for supporting this research. A.R. and M.P. thank the FIRENZE HYDROLAB project by Ente Cassa di Risparmio di Firenze for sponsoring this research activity.

REFERENCES

(1) Li, H.-W.; Yan, Y.; Orimo, S.-i.; Züttel, A.; Jensen, C. M. *Energies* **2011**, *4*, 185.
(2) Guo, Y.; Yu, X.; Sun, W.; Sun, D.; Yang, W. *Angew. Chem., Int. Ed.* **2011**, *50*, 1087.
(3) Ingleson, M. J.; Barrio, J. P.; Bacsa, J.; Steiner, A.; Darling, G. R.; Jones, J. T. A.; Khimyak, Y. Z.; Rosseinsky, M. J. *Angew. Chem., Int. Ed.* **2009**, *48*, 2012.
(4) Soloveichik, G.; Her, J.-H.; Stephens, P. W.; Gao, Y.; Rijssenbeek, J.; Andrus, M.; Zhao, J. C. *Inorg. Chem.* **2008**, *47*, 4290.
(5) Fleet, G. W. J.; Harding, P. J. C. *Tetrahedron Lett.* **1981**, *22*, 675.
(6) Sorrell, T. N.; Pearlman, P. S. *J. Org. Chem.* **1980**, *45*, 3449.
(7) Fleet, G. W. J.; Harding, P. J. C.; Whitcombe, M. J. *Tetrahedron Lett.* **1980**, *21*, 4031.
(8) Bhanushali, M. J.; Nandurkar, N. S.; Bhor, M. D.; Bhanage, B. M. *Tetrahedron Lett.* **2007**, *48*, 1273.
(9) Gysling, H. J.; Vinal, R. S. Photographic Systems Based on Photosensitive Copper(I) Complexes. U.S. Patent 3,859,092, January 7, 1975.
(10) Grutsch, P. A.; Kutal, C. *J. Am. Chem. Soc.* **1977**, *99*, 6460.
(11) Grutsch, P. A.; Kutal, C. *J. Am. Chem. Soc.* **1979**, *101*, 4228.
(12) Marks, T. J.; Kolb, J. R. *Chem. Rev.* **1977**, *77*, 263.
(13) Xu, Z.; Lin, Z. *Coord. Chem. Rev.* **1996**, *156*, 139.
(14) Makhaev, V. D. *Russ. Chem. Rev.* **2000**, *69*, 727.
(15) Besora, M.; Lledós, A. In *Complexes Contemporary Metal Boron Chemistry I*; Marder, T., Lin, Z., Eds.; Springer: Berlin/Heidelberg, 2008; Vol. *130*, p 149.
(16) Sewell, L. J.; Lloyd-Jones, G. C.; Weller, A. S. *J. Am. Chem. Soc.* **2012**, *134*, 3598.
(17) Stevens, C. J.; Dallanegra, R.; Chaplin, A. B.; Weller, A. S.; Macgregor, S. A.; Ward, B.; McKay, D.; Alcaraz, G.; Sabo-Etienne, S. *Chem.—Eur. J.* **2011**, *17*, 3011.
(18) Johnson, H. C.; Robertson, A. P. M.; Chaplin, A. B.; Sewell, L. J.; Thompson, A. L.; Haddow, M. F.; Manners, I.; Weller, A. S. *J. Am. Chem. Soc.* **2011**, *133*, 11076.
(19) Filippov, O. A.; Filin, A. M.; Tsupreva, V. N.; Belkova, N. V.; Lledós, A.; Ujaque, G.; Epstein, L. M.; Shubina, E. S. *Inorg. Chem.* **2006**, *45*, 3086.

(20) Desrosiers, P. J.; Cai, L.; Lin, Z.; Richards, R.; Halpern, J. *J. Am. Chem. Soc.* **1991**, *113*, 4173.
(21) Bakhmutov, V. I. *Dihydrogen Bonds: Principles, Experiments, and Applications*; John Wiley & Sons, Inc.: Hoboken, NJ, 2008.
(22) Cariati, F.; Naldini, L. *Gazz. Chim. Ital.* **1965**, *95*, 3.
(23) Rossin, A.; Peruzzini, M.; Zanobini, F. *Dalton Trans.* **2011**, *40*, 4447.
(24) Frisch, M. J.; Trucks, G. W.; Schlegel, H. B.; Scuseria, G. E.; Robb, M. A.; Cheeseman, J. R.; Scalmani, G.; Barone, V.; Mennucci, B.; Petersson, G. A.; Nakatsuji, H.; Caricato, M.; Li, X.; Hratchian, H. P.; Izmaylov, A. F.; Bloino, J.; Zheng, G.; Sonnenberg, J. L.; Hada, M.; Ehara, M.; Toyota, K.; Fukuda, R.; Hasegawa, J.; Ishida, M.; Nakajima, T.; Honda, Y.; Kitao, O.; Nakai, H.; Vreven, T.; Montgomery, J. A.; Peralta, J. E.; Ogliaro, F.; Bearpark, M.; Heyd, J. J.; Brothers, E.; Kudin, K. N.; Staroverov, V. N.; Kobayashi, R.; Normand, J.; Raghavachari, K.; Rendell, A.; Burant, J. C.; Iyengar, S. S.; Tomasi, J.; Cossi, M.; Rega, N.; Millam, J. M.; Klene, M.; Knox, J. E.; Cross, J. B.; Bakken, V.; Adamo, C.; Jaramillo, J.; Gomperts, R.; Stratmann, R. E.; Yazyev, O.; Austin, A. J.; Cammi, R.; Pomelli, C.; Ochterski, J. W.; Martin, R. L.; Morokuma, K.; Zakrzewski, V. G.; Voth, G. A.; Salvador, P.; Dannenberg, J. J.; Dapprich, S.; Daniels, A. D.; Farkas, J. B.; Foresman, J. V.; Ortiz, J. V.; Cioslowski, J.; Fox, D. J. *Gaussian09*; Gaussian, Inc.: Wallingford, CT, 2009.
(25) Zhao, Y.; Truhlar, D. *Theor. Chim. Acta* **2008**, *120*, 215.
(26) Swart, M.; Güell, M.; Luis, J. M.; Solà, M. *J. Phys. Chem. A* **2010**, *114*, 7191.
(27) Krishnan, R.; Binkley, J. S.; Seeger, R.; Pople, J. A. *J. Chem. Phys.* **1980**, *72*, 650.
(28) Hehre, W. J.; Ditchfield, R.; Pople, J. A. *J. Chem. Phys.* **1972**, *56*, 2257.
(29) Dill, J. D.; Pople, J. A. *J. Chem. Phys.* **1975**, *62*.
(30) Fritsch, J.; Zundel, G. *J. Phys. Chem.* **1981**, *85*, 556.
(31) Kramer, R.; Zundel, G. *J. Chem. Soc., Faraday Trans.* **1990**, *86*, 301.
(32) Wiberg, K. B. *Tetrahedron* **1968**, *24*, 1083.
(33) Reed, A. E.; Curtiss, L. A.; Weinhold, F. *Chem. Rev.* **1988**, *88*, 899.
(34) Glendening, E. D.; Badenhoop, J. K.; Reed, A. E.; Carpenter, J. E.; Bohman, J. A.; Morales, C.; Weindhold, F.*NBO 5.0*; Theoretical Chemistry Institute, University of Wisconsin: Madison, WI, 2001.
(35) Keith, T. A. *AIMALL*; TK Gristmill Software: Overland Park, KS, 2011.
(36) Espinosa, E.; Molins, E.; Lecomte, C. *Chem. Phys. Lett.* **1998**, *285*, 170.
(37) Espinosa, E.; Alkorta, I.; Rozas, I.; Elguero, J.; Molins, E. *Chem. Phys. Lett.* **2001**, *336*, 457.
(38) Bader, R. F. W. *Atoms in Molecules: A Quantum Theory (International Series of Monographs on Chemistry)*; Oxford University Press: New York, 1994.
(39) Popelier, P. L. *Atoms in Molecules: An Introduction*; Prentice Hall: London, 2000.
(40) Matta, C.; Boyd, R. J. *Quantum Theory of Atoms in Molecules: Recent Progress in Theory and Application*; Wiley-VCH: New York, 2007.
(41) Boys, S. F.; Bernardi, F. *Mol. Phys.* **1970**, *19*, 553.
(42) Tuma, C.; Boese, D. A.; Handy, N. C. *Phys. Chem. Chem. Phys.* **1999**, *1*, 3939.
(43) Buemi, G. Intramolecular Hydrogen Bonds. In *Methodologies and Strategies for Their Strength Evaluation Hydrogen Bonding—New Insights*; Grabowski, S., Ed.; Springer: Amsterdam, The Netherlands, 2006; pp 51−107.
(44) Marenich, A. V.; Cramer, C. J.; Truhlar, D. G. *J. Phys. Chem. B* **2009**, *113*, 6378.
(45) Sumimoto, M.; Iwane, N.; Takahama, T.; Sakaki, S. *J. Am. Chem. Soc.* **2004**, *126*, 10457.
(46) Jeffrey, G. A. *An Introduction to Hydrogen Bonding (Topics in Physical Chemistry)*; Oxford University Press: New York, 1997.
(47) Belkova, N. V.; Shubina, E. S.; Epstein, L. M. *Acc. Chem. Res.* **2005**, *38*, 624.
(48) Grabowski, S. J.; Sokalski, W. A.; Leszczynski, J. *J. Phys. Chem. A* **2005**, *109*, 4331.
(49) Cioslowski, J.; Mixon, S. T.; Edwards, W. D. *J. Am. Chem. Soc.* **1991**, *113*, 1083.
(50) Koch, U.; Popelier, P. L. A. *J. Phys. Chem.* **1995**, *99*, 9747.
(51) Rozas, I.; Alkorta, I.; Elguero, J. *J. Phys. Chem. A* **1998**, *102*, 9925.
(52) Pacios, L. F. *J. Comput. Chem.* **2006**, *27*, 1641.
(53) Rozas, I. *Phys. Chem. Chem. Phys.* **2007**, *9*, 2782.
(54) Kulkarni, S. A. *J. Phys. Chem. A* **1998**, *102*, 7704.
(55) Kulkarni, S. A.; Srivastava, A. K. *J. Phys. Chem. A* **1999**, *103*, 2836.
(56) Grabowski, S. J. *Chem. Rev.* **2011**, *111*, 2597.
(57) Belkova, N. V.; Besora, M.; Baya, M.; Dub, P. A.; Epstein, L. M.; Lledós, A.; Poli, R.; Revin, P. O.; Shubina, E. S. *Chem.—Eur. J.* **2008**, *14*, 9921.
(58) Dub, P. A.; Belkova, N. V.; Filippov, O. A.; Daran, J.-C.; Epstein, L. M.; Lledós, A.; Shubina, E. S.; Poli, R. *Chem.—Eur. J.* **2010**, *16*, 189.
(59) Iogansen, A. V. *Theor. Experim. Khim.* **1971**, *7*, 302.
(60) Iogansen, A. V. *Theor. Experim. Khim.* **1971**, *7*, 314.
(61) Filippov, O. A.; Filin, A. M.; Teplitskaya, L. N.; Belkova, N. V.; Shmyrova, Y. V.; Sivaev, I. B.; Bregadze, V. I.; Epstein, L. M.; Shubina, E. S. *Main Group Chem.* **2005**, *4*, 97.
(62) Makhaev, V. D.; Borisov, A. P.; Lobkovskii, É. B.; Polyakova, V. B.; Semenenko, K. N. *Russ. Chem. Bull.* **1985**, *34*, 1731.
(63) Belkova, N. V.; Filippov, O. A.; Filin, A. M.; Teplitskaya, L. N.; Shmyrova, Y. V.; Gavrilenko, V. V.; Golubinskaya, L. M.; Bregadze, V. I.; Epstein, L. M.; Shubina, E. S. *Eur. J. Inorg. Chem.* **2004**, *2004*, 3453.
(64) Filippov, O. A.; Tsupreva, V. N.; Golubinskaya, L. M.; Krylova, A. I.; Bregadze, V. I.; Lledos, A.; Epstein, L. M.; Shubina, E. S. *Inorg. Chem.* **2009**, *48*, 3667.
(65) Iogansen, A. V. *The Hydrogen Bond*; Nauka: Moscow, 1981.
(66) Iogansen, A. V. *Spectrochim. Acta, Part A* **1999**, *55*, 1585.
(67) Epstein, L. M.; Shubina, E. S.; Bakhmutova, E. V.; Saitkulova, L. N.; Bakhmutov, V. I.; Chistyakov, A. L.; Stankevich, I. V. *Inorg. Chem.* **1998**, *37*, 3013.
(68) Belkova, N. V.; Epstein, L. M.; Shubina, E. S. *Eur. J. Inorg. Chem.* **2010**, *2010*, 3555.
(69) Shubina, E. S.; Bakhmutova, E. V.; Filin, A. M.; Sivaev, I. B.; Teplitskaya, L. N.; Chistyakov, A. L.; Stankevich, I. V.; Bakhmutov, V. I.; Bregadze, V. I.; Epstein, L. M. *J. Organomet. Chem.* **2002**, *657*, 155.
(70) Sivaev, I. B.; Bragin, V. I.; Prikaznov, A. V.; Petrovskii, P. V.; Bregadze, V. I.; Filippov, O. A.; Teplinskaya, T. A.; Titov, A. A.; Shubina, E. S. *Collect. Czech. Chem. Commun.* **2007**, *72*, 1725.
(71) Filippov, O. A.; Filin, A. M.; Belkova, N. V.; Tsupreva, V. N.; Shmyrova, Y. V.; Sivaev, I. B.; Epstein, L. M.; Shubina, E. S. *J. Mol. Struct.* **2006**, *790*, 114.
(72) Cariati, F.; Naldini, L. *J. Inorg. Nucl. Chem.* **1966**, *28*, 2243.
(73) Green, B. E.; Kennard, C. H. L.; Smith, G.; James, B. D.; Healy, P. C.; White, A. H. *Inorg. Chim. Acta* **1984**, *81*, 147.
(74) Knizek, J.; Nöth, H.; Warchhold, M. *Z. Naturforsch..B* **2006**, *61*, 1079.
(75) Golden, J. H.; Schreier, C.; Singaram, B.; Williamson, S. M. *Inorg. Chem.* **1992**, *31*, 1533.
(76) Mesmer, R. E.; Jolly, W. L. *Inorg. Chem.* **1962**, *1*, 608.
(77) Maseras, F.; Lledós, A.; Clot, E.; Eisenstein, O. *Chem. Rev.* **2000**, *100*, 601.
(78) Rappoport, Z. *The Chemistry of Phenols (Chemistry of Functional Groups)*; John Wiley & Sons: Jerusalem, 2003; Part 2.
(79) Huey, L. G.; Dunlea, E. J.; Howard, C. J. *J. Phys. Chem.* **1996**, *100*, 6504.
(80) Tague, T. J.; Andrews, L. *J. Am. Chem. Soc.* **1994**, *116*, 4970.
(81) Schreiner, P. R.; Schaefer, H. F.; Schleyer, P. v. R. *J. Chem. Phys.* **1994**, *101*, 7625.
(82) Watts, J. D.; Bartlett, R. J. *J. Am. Chem. Soc.* **1995**, *117*, 825.
(83) Esteruelas, M. A.; Garcia, M. P.; Lopez, A. M.; Oro, L. A.; Ruiz, N.; Schluenken, C.; Valero, C.; Werner, H. *Inorg. Chem.* **1992**, *31*, 5580.

(84) Rhodes, L. F.; Venanzi, L. M.; Sorato, C.; Albinati, A. *Inorg. Chem.* **1986**, *25*, 3335.
(85) Hillier, A. C.; Jacobsen, H.; Gusev, D.; Schmalle, H. W.; Berke, H. *Inorg. Chem.* **2001**, *40*, 6334.
(86) Guilera, G.; McGrady, S. G.; Steed, J. W.; Kaltsoyannis, N. *New J. Chem.* **2004**, *28*, 444.